Journal of Cellular Biochemistry 89:808–823 (2003)

Increased Expression of Disintegrin-Metalloproteinases ADAM-15 and ADAM-9 Following Upregulation of Integrins α5β1 and αvβ3 in Atherosclerosis

Nadia Al-Fakhri,[1]* Jochen Wilhelm,[2] Meinhard Hahn,[2] Martin Heidt,[3] Friedrich W. Hehrlein,[3] Andrea M. Endisch,[4] Thomas Hupp,[4] Sanjay M. Cherian,[5] Yuri V. Bobryshev,[5] Reginald S.A. Lord,[5] and Norbert Katz[1]

[1]Institute of Clinical Chemistry and Pathobiochemistry, Justus Liebig University, Giessen, Germany
[2]Institute of Biochemistry, Justus Liebig University, Giessen, Germany
[3]Clinic for Cardiovascular Surgery, Justus Liebig University, Giessen, Germany
[4]Clinic for Vascular Surgery, Katharinenhospital, Stuttgart, Germany
[5]Surgical Professorial Unit, St. Vincent's Hospital, University of New South Wales, Sydney, Australia

Abstract Regulation of αvβ3 and α5β1 integrin function plays a crucial role in atherosclerosis. Possible regulators of integrin–matrix interactions are integrin-binding ADAMs (proteins with a disintegrin- and metalloproteinase-domain), like ADAM-15 and ADAM-9. Molecular interactions between ADAM-15, α5β1, and αvβ3 have been demonstrated. ADAM-9 and ADAM-15 were found to be interdependently regulated. This study, therefore, investigated whether the upregulation of integrins α5β1 and αvβ3 was correlated with the expression of integrin-binding ADAMs in atherosclerotic processes. Human arterial and venous vascular smooth muscle cells (VSMCs) were incubated with PDGF over different time intervals up to a 3-day culture period. mRNA concentrations, quantified by real-time RT-PCR and normalized to PBGD, of integrins αvβ3 and α5β1 were strongly increased after a 12-h PDGF-incubation in arterial and venous VSMC. ADAM-15 and ADAM-9 mRNA production showed a corresponding increase following integrin upregulation after a 24-h incubation period. Western blot anaylsis revealed an increased protein expression of integrins and ADAMs in PDGF-stimulated VSMC. Additionally, mRNA concentrations of atherosclerotic and normal human specimens were quantified by real-time RT-PCR. mRNA of ADAMs and integrins was significantly increased in atherosclerotic arteries compared to normal arteries. Immunohistochemistry of these specimens showed an increased expression and codistribution of both ADAMs and integrins in atherosclerosis. In conclusion, upregulation of ADAM-15 and ADAM-9 in atherosclerosis appears to follow an increase in α5β1 and αvβ3 integrins. Since α5β1 and αvβ3 are known to promote smooth muscle cell migration and proliferation, upregulation of ADAM-15 and ADAM-9 could balance integrin–matrix interactions and cell migration, thus modulating neointima progression. J. Cell. Biochem. 89: 808–823, 2003.

Key words: ADAMs; integrins; atherosclerosis; neointima; smooth muscle cells; PDGF

Abbreviations used: α5, αv, β1, β3, integrin subunits; ADAM, protein with a disintegrin- and metalloproteinase-domain; asp, anti-sense primer; bp, base pairs; cDNA, complementary DNA; dsDNA, double-stranded DNA; ssDNA, single-stranded DNA; EGF-domain, epidermal growth factor-like domain; LC, LightCycler technology (Roche Diagnostics, Basel, Switzerland); mRNA, messenger ribonucleic acid; OD_{260}, ratio of spectrophotometric optical density at 260 nm; PBGD, non-erythropoietic porphobilinogen-deaminase; PCR, polymerase chain reaction; PDGF, platelet-derived growth factor; RGD-motif, amino acid sequence arginine-glycine-aspartic acid; RT, reverse transcription; sp, sense primer.

Grant sponsor: Deutsche Forschungsgemeinschaft, Bonn, Germany; Grant number: AL 460/2-1; Grant sponsor: German Society for Vascular Surgery, Heidelberg, Germany (Research Rewards); Grant sponsor: German Society for Arteriosclerosis Research, Tübingen, Germany (Research Rewards) (to NA).

Dr. Meinhard Hahn's present address is Division of Molecular Genetics, Deutsches Krebsforschungszentrum, Heidelberg, Germany.

*Correspondence to: Dr. Nadia Al-Fakhri, Institute of Clinical Chemistry and Pathobiochemistry, Justus Liebig University, Gaffkystraße 11, 35392 Giessen, Germany.
E-mail: nadia.al-fakhri@klinchemie.med.uni-giessen.de

Received 13 November 2002; Accepted 17 March 2003
DOI 10.1002/jcb.10550

In atherosclerosis, cell–matrix interactions have a major influence on neointima formation [Al-Fakhri et al., 1997; Raines et al., 2000; Moiseeva, 2001]. Integrins mediate cell–matrix interactions that modulate cell spreading, migration, and adhesion [Moiseeva, 2001] and determine neointima progression. However, the regulation of integrin function has not been entirely clarified. Integrins constitute a family of membrane-anchored cell-adhesion receptors that transduce extracellular signals to the cytoskeleton and to signal transduction pathways. They consist of different α- and β- subunits according to which various integrin subfamilies have been defined [Isacke and Horton, 2000; Moiseeva, 2001]. Integrin binding evokes cellular responses ranging from inhibition to stimulation of smooth muscle cell migration depending on the binding partner [Werb et al., 1989; Moiseeva, 2001]. Interaction of several matrix- and possibly also cell-bound ligands governs the fine-regulation of integrins.

Understanding integrin regulation in neointima formation may result from investigations on ADAMs (proteins with a disintegrin- and metalloproteinase-domain), possible modulators of integrin function according to their molecular structure [Blobel, 1997]. ADAMs are a family of cell surface molecules consisting primarily of membrane-bound proteins (58–99 kDa) with multiple domains, that link to the family of membrane-bound proteinases [Wolfsberg et al., 1995; Huovila et al., 1996; Huang, 1998; Stone et al., 1999]. ADAMs are involved in various cellular processes that include cell fusion, proteolysis, cell adhesion, signal transduction, and ectodomain shedding [Huovila et al., 1996; Blobel, 1997; Flannery et al., 1999]. The domains of membrane-anchored ADAMs exhibit various other functions, among them an integrin-binding function through the disintegrin-domain [Wolfsberg et al., 1995; Stone et al., 1999]. Based on their domain characteristics, it has been postulated that ADAMs function as integrin regulators on the same cell or on neighboring cells and may alter interactions with matrix substances [Blobel, 1997; Herren et al., 1997].

The integrins αvβ3 and α5β1 that are investigated in this report are prominently related to atherosclerosis development and progression [Veinot et al., 1999; Ikari et al., 2000; Davenpeck et al., 2001; Moiseeva, 2001]. They both recognize a functional RGD-motif (Arg-Gly-Asp) of their ligand, a characteristic common to most extracellular matrix proteins [Isacke and Horton, 2000] and to several ADAMs with a functional disintegrin-domain [Wolfsberg et al., 1995; Stone et al., 1999]. Ligand specificity of integrins differs not only between integrin subfamilies, but also within the same integrin depending on ligand and integrin conformity [Isacke and Horton, 2000; Moiseeva, 2001]. Therefore, α5β1 is mainly a fibronectin-receptor and αvβ3 mainly a vitronectin-receptor, but various other ligands have been described [Isacke and Horton, 2000]. Molecular interactions demonstrated between integrins and integrin-binding ADAMs, such as ADAM-9 (synonymous MDC-9) and ADAM-15 (MDC-15, metargidin), suggest a role for ADAMs as integrin ligands and regulators in vivo. ADAM-15 is a ligand of integrins αvβ3 and α5β1; it enhances intercellular adhesion and reduces migration [Zhang et al., 1998, 1999; Herren et al., 2001]. ADAM-9 has been shown to bind to different integrin receptors and promote migration [Nath et al., 2000; Zhou et al., 2001]. ADAM-9 and ADAM-15 influence adhesion and cell–cell interactions through integrin binding [Eto et al., 2000; Zhou et al., 2001]. Furthermore, ADAM-9 and ADAM-15 have been described to be differentially regulated: ADAM-9 mRNA is downregulated, while ADAM-15 mRNA is upregulated in a chondrocyte model of inflammation [Flannery et al., 1999]. ADAM-15 may play a role in atherosclerosis development, as demonstrated in an animal model [Herren et al., 1997].

It has so far not been investigated, whether the upregulation of integrins α5β1 and αvβ3 in atherosclerosis was paralleled by a change in the expression of integrin-binding ADAMs that could point to a related regulation. The present study investigated related changes of ADAM-9, ADAM-15, integrins αvβ3 and α5β1 mRNA production, and protein expression in growth factor stimulated and non-stimulated VSMC as well as in human atherosclerotic and normal vessels.

MATERIALS AND METHODS

Cell Culture

Human arterial and venous vascular smooth muscle cell (VSMC) cultures were obtained from human saphenous vein and internal mammary artery segments, explanted, and prepared as

previously described [Huang et al., 2002]. VSMCs were isolated from the medial tissue of vessel segments after trypsin digestion, grown to confluency in DMEM culture medium supplemented with 10% fetal calf serum (Gibco, Paisley, Scotland), penicillin (100 U/ml), streptomycin (100 μg/ml), and amphotericin B (0.025 μg/ml) (all from Sigma, St. Louis, MO). Cultures were maintained at 37°C in a humidified atmosphere with 5% (v/v) CO_2 in air. VSMCs from veins and arteries were separately cultured. Confluent VSMCs were detached with trypsin 2.5 mg/ml that was subsequently neutralized with soybean trypsin inhibitor 40 μg/ml (Sigma) and washed in serum-free medium. 10^6 cells/ml were distributed onto plates. Cells were incubated for culture periods from 6 h to 3 days (6, 12, 24 h and 2 or 3 days) in the absence or presence of 10 ng/ml platelet-derived growth factor-BB (PDGF) (Sigma). The PDGF concentration employed was according to previous studies [Huang et al., 2002]. Individual plates were analyzed immediately at the beginning of the incubation (time point 0). Cells were harvested by trypsinization, as described above, and subjected to RNA and protein isolation. Arterial and venous VSMC incubated in the presence or absence of 10 ng/ml PDGF over a 3-day culture period were subjected to real-time PCR to investigate ADAM-9, ADAM-15, integrins α5β1, and αvβ3 mRNA production. PDGF-stimulated VSMCs analyzed at different time points during cell culture (0, 6, 12, 24 h, 2 and 3 days) were also subjected to real-time RT-PCR to determine sequential changes in integrin and ADAM mRNA production. Protein expression was analyzed by Western blot.

Human Arterial Specimens

Atherosclerotic tissue was obtained from 13 carotid artery specimens collected during carotid eversion endarterectomy of 12 patients with uni- or bi-lateral carotid artery stenosis. Specimens consisted of neointima and media tissue. Patient mean age was 63.8 years (range: 49–76 years), 7 men and 5 women. For patient characteristics see Table I. Controls consisted of normal thyroid artery specimens from eight pre-menopausal women, mean age 42.4 years (range: 32–49 years), collected during thyroid operations. Only the media and intima tissue was processed. The women had no known cardiovascular or metabolic disorder; patients with autoimmune thyroiditis and thyroid cancer were excluded. Additionally, thyroid arteries of three women (aged 68, 71, and 81 years) with known generalized atherosclerosis were collected. The study was approved by the Ethical Committee of Justus Liebig University Giessen; all subjects gave informed consent. Normal and atherosclerotic human specimens were analyzed by real-time RT-PCR for differences in integrin and ADAM mRNA production. Protein expression was investigated by immunohistochemistry.

TABLE I. Patient Characteristics

Stage of cerebro-vascular insufficiency
Stage I (asymptomatic) 11/13 operations
Stage II (TIA) 2/13 op.
Stage III (PRIND) 0/13 op.
Stage IV (stroke) 0/13 op.
Atherosclerosis risk factors
Hypertension 8/12 patients
Hypercholesterolemia 8/12 pat.
Cigarette smoking 6/12 pat.
Diabetes mellitus 4/12 pat.
Hyperuricemia 4/12 pat.
Preoperative medication
ASA 6/12 patients
Anti-cholesteremics 5/12 pat.
Anti-coagulants (heparin, phenprocoumon, thienopyridines) 5/12 pat.
Nitrates 4/12 pat.
Calcium-antagonists 4/12 pat.
ACE inhibitors 4/12 pat.
Beta-receptor blockers 3/12 pat.
Diuretics 3/12 pat.
Insulin 1/12 pat.

Patient characteristics of 13 atherosclerotic specimens from carotid arteries collected during eversion endarterectomy of 13 patients with uni- or bi-lateral carotid artery stenosis.
PRIND, prolonged reversible ischemic neurologic deficits; TIA, transient ischemic attack; ACE, angiotensin converting enzyme, ASA, acetyl-salicylic acid.

RNA Preparation

Specimens were directly processed under sterile conditions, frozen in liquid nitrogen, homogenized manually, and lysed in 500 μl Trizol (Sigma). Total cellular RNA was extracted using a modified single-step isolation protocol based on established methods [Chomczynski and Sacchi, 1987]. RNA concentrations were calculated on the basis of OD_{260} using Ultrospec III spectrophotometer (Pharmacia, Amersham Pharmacia, Piscataway, NJ). Final RNA concentrations were between 0.3 and 3.4 μg/μl.

Reverse Transcription (RT) of RNA

Genomic DNA contamination was eliminated by a protocol adapted from described methods [Hanaki et al., 2000; Wiame et al., 2000]. The solution containing 1 μg/μl RNA was incubated

for 30 min at 37°C with 0.09 U/μl RNAse-free DNAse (Promega, Madison, WI), 40 U RNAse inhibitors (RNAsin, Promega), and 0.66 mM $MnCl_2$ in 10 mM Tris-HCl pH 7.8 in a volume of 11 μl. Prior to heat inactivation of DNAse at 75°C for 5 min, 3 mM EDTA and 0.15 mM DTT were added to avoid subsequent DNAse reactivation [Hanaki et al., 2000]. Subsequently, the reaction mixture was cooled to 42°C. RT was performed at 42°C for 60 min after addition of 8 U avian myeloblastosis virus (AMV) reverse transcriptase, 10.55 mmol/L DTT, 11.34 mmol/L $MgCl_2$, 0.57 μg oligo-dT primer, 0.5 mmol/L dNTP's, and 32 U RNAse inhibitors (reverse transcription system, Promega) in a total volume of 21 μl. The reaction was terminated by heat inactivation of reverse transcriptase at 90°C for 5 min. RT products were diluted to 10 ng cDNA/μl in sterile Aqua dest. for subsequent polymerase chain reaction (PCR).

Synthesis of PCR External Standards

Primer pairs used were derived from the target cDNA sequence upstream and downstream of the real-time PCR primers (Table II). For external standards, PCR was performed in 20 μl final volume containing 20 ng cDNA of a defined specimen, 0.2 mmol/L dNTP-Mix (Amersham Pharmacia), 0.5 U Taq DNA-Polymerase (Eppendorf, Hamburg, Germany), 10 pmol of each primer (synthesized by MWG-Biotech, Ebersberg, Germany), 50 mmol/L KCl in 10 mmol/L Tris-HCl pH 8.3, and 1.5 mmol/L $MgCl_2$. Individual PCR protocols were employed for every PCR target. PCR products were electrophoresed in 2% NA agarose gels (Amersham Pharmacia). Specific products were identified after ethidium-bromide staining under ultraviolet light, excised from the gel and extracted with Qiaex II agarose gel extraction kit (Qiagen, Germantown, MD). The concentrations of the DNA standards were adjusted to 5×10^9 amplicons/μl in 2 mM Tris-HCl pH 7.8 buffer containing the same amount of $MnCl_2$, $MgCl_2$, DTT, and EDTA as the cDNA preparation from the RT procedure.

Real-Time Polymerase Chain Reaction (PCR)

For real-time PCR, we used the LightCycler (LC) (Roche Diagnostics, Basel, Switzerland). The principle has been described previously [Wilhelm et al., 2000]. Briefly, the quantification is based on monitoring PCR product accumulation in real-time during the entire PCR cycling by fluorescense detection of the dsDNA-specific dye SYBR Green I (Roche Diagnostics). Immediately before PCR, 0.5 U *Taq* DNA polymerase were pre-incubated for 10 min at 25°C with 1.1 μg anti-*Taq* DNA polymerase antibody (TaqStart antibody, Sigma) to avoid amplification of non-specific products. Real-time PCR was performed in 10 μl final volume of reaction mixture containing 20 ng cDNA, a 1:100,000 dilution of SYBR Green I, 0.5 g/L bovine serum albumin (Amersham Pharmacia), 0.2 mmol/L dNTP-Mix (Amersham Pharmacia), 0.5 U Taq DNA-Polymerase (Eppendorf), 5 pmol of each primer (Table II) (synthesized by MWG-Biotech), 5 mmol/L $MgCl_2$ and 50 mmol/L KCl in 10 mmol/L Tris-HCl pH 8.3. The optimal $MgCl_2$ concentrations were determined in preceding

TABLE II. Primer Pairs for Standards and Real-Time PCR

Target (mRNA)	Acc. no. (GenBank)	Primer pairs used for standards and LC-PCR
ADAM-9	U41766	S: sp 436-464 asp 1450-1479 (1044 bp) LC: sp 1208-1227 asp 1316-1334 (127 bp)
ADAM-15	U46005	S: sp 1429-1456 asp 1821-1849 (421 bp) LC: sp 1597-1615 asp 1743-1762 (166 bp)
α5	X06256	S: sp 597-614 asp 994-1011 (415 bp) LC: sp 804-820 asp 867-886 (83 bp)
αv	M14648	S: sp 274-291 asp 576-593 (320 bp) LC: sp 284-299 asp 366-385 (102 bp)
β1	X07979	S: sp 414-431 asp 925-942 (529 bp) LC: sp 627-646 asp 725-742 (116 bp)
β3	J02703	S: sp 1507-1524 asp 2004-2021 (515 bp) LC: sp 1845-1864 asp 1951-1968 (124 bp)
PBGD	X04808	S: sp 28-46 asp 427-446 (419 bp) LC: sp 63-83 asp 188-206 (144 bp)

Primer pairs used for PCR external standard generation (S) and for real-time PCR in the LightCycler (LC) system are given for every individual target mRNA. Primers are defined according to the nucleotide numbers of the mRNA sequence as deposited in the GenBank; primer pairs consist of sense primer (sp) and antisense primers (asp). Standard and real-time PCR product sizes are given in parentheses. Primer sequences were deduced from human mRNA sequences. Oligo 5.0 software (National Biosciences) was used to check for the absense of false priming sites, formation of primer dimers, and secondary structures.

experiments. Negative controls were conducted by omitting cDNA in the reaction mixture. Reagents and LC capillaries were cooled during preparation of the reaction mixture until the start of PCR. In parallel to the individual runs of every target, we conducted PCR reactions of external standards of the same target sequence in defined 1:5 dilution series from 5×10^4 to 1×10^0. The external standards yielded corresponding standard curves that covered the curves of VSMC and human specimens.

Individual PCR protocols were employed for every target that was optimized for a high signal-to-noise ratio. For ADAM-9, 5 min 95°C followed by 50 cycles: 1 s 95°C, 5 s 56°C, 5 s 72°C. ADAM-15: 5 min 94°C, 50 cycles: 5 s 94°C, 10 s 61°C, 10 s 72°C. αv: 5 min 95°C, 50 cycles: 5 s 95°C, 10 s 56°C, 10 s 72°C. α5: 5 min 95°C, 50 cycles: 1 s 95°C, 5 s 56°C, 10 s 72°C. β1: 5 min 95°C, 50 cycles: 1 s 95°C, 5 s 55°C, 10 s 72°C. β3: 5 min 95°C, 50 cycles: 1 s 95°C, 5 s 56°C, 5 s 72°C. For the house keeping gene *PBGD* (non-erythropoietic porphobilinogen deaminase): 5 min 95°C, 50 cycles: 5 s 95°C, 10 s 57°C, 10 s 72°C. Immediately at the end of the final extension phase, continuous fluorescence measurements were taken while the temperature was increased from 72 up to 95°C with a ramp of 0.1°C/s. Hereby, the obtained PCR products were characterized in a melting curve analysis. The correlation of melting curves and product lengths was examined by performing electrophoreses on 8% polyacrylamide gels as well as on 2% NA agarose gels (Amersham Pharmacia). This demonstrated the presence of the specific products and excluded nonspecific products or primer dimers.

LC Data Evaluation

Data were evaluated with the LC software, version 3.0 that calculated the amount of initial target copies/μl with the aid of the threshold cycle (C_T) values and according to the given external standard curve in each real-time PCR run. The final amount of mRNA copies/μl was calculated by duplicating the results for cDNA copies/μl to adjust for the different amounts of DNA strands between cDNA samples (ssDNA) and standards (dsDNA) at the start of real-time PCR. The results given in copies/μl were normalized to the results of PBGD-mRNA in copies/μl and reported as mean values of mRNA copies/PBGD-mRNA copy. Data from VSMC were obtained from three independent experiments measured in duplicate. Data from human specimens were obtained from three consecutive measurements. Differences between atherosclerotic and normal specimens or between VSMC cultured with or without PDGF for different culture periods were tested for significance using student's *t*-test. Differences for every target were considered significant, if P was less than 0.05.

Western Blot

Cells were homogenized on ice, total protein was isolated through methanol–chloroform precipitation and transferred to Lämmli's buffer containing protease inhibitors (Roche Diagnostics). Thirty micrograms of each protein sample were electrophoresed on 12% polyacrylamide gels, and then transferred to a blot membrane (Millipore, Bedford, MA) at 125 mA in 105 min. The membrane was blocked with 5% fish gelatine and incubated with the primary antibody for 4 h at RT. Polyclonal rabbit antibodies against ADAM-9 (Chemicon, Temecula, CA, 1:500) and ADAM-15 (Chemicon, 1:400) or monoclonal mouse antibodies against α5β1 (JBS5, Chemicon, 1:1,000) and αvβ3 (LM609, Chemicon, 1:1,000) were employed. The blot membrane was rinsed, incubated with the secondary horseradish-peroxidase conjugated anti-mouse- or anti-rabbit-antibodies, rinsed again, and developed with enhanced chemiluminescence (LumiLight, Roche Diagnostics).

Immunohistochemistry

Specimens were fixed with 4% formaldehyde, paraffin embedded, cut in 6 μm serial sections on a Leica SM2400 microtome, mounted on gelatin-coated slides, and deparaffinized. Individual sections were stained with hematoxylin-eosin for conventional light microscopy as a reference to immunohistochemical analysis. Slides were pre-incubated with 5% normal goat serum, then incubated with polyclonal rabbit antiserum against ADAM-9 (against disintegrin domain, Chemicon, 1:250) and ADAM-15 (against carboxyterminal region, Chemicon, 1:200) or with monoclonal mouse antibodies against α5β1 (JBS5, Chemicon, 1:700), αvβ3 (LM609, Chemicon, 1:700), smooth muscle α-actin (1A4, Dako, Glostrup, Denmark, 1:100), macrophage-antigen CD68 (KP1, Dako, 1:100), T-lymphocyte antigen CD3 (T3-4B5, Dako, 1:100), and B-lymphocyte antigen CD21 (1F8,

Dako, 1:100). In prior experiments, all antibodies had been tested for applicability to paraffin embedded tissue by comparison to acetone fixed cryostate sections of atherosclerotic tissue. Negative controls were conducted by substituting the specific primary antibody through an irrelevant antibody. Ensuing incubations were carried out with biotinylated goat-anti-rabbit or goat-anti-mouse antibodies, streptavidin-alkaline phosphatase-conjugate, Fast Red TR/Naphthol AS-MX staining (Sigma), and Mayer's hemalum counterstaining. Slides were covered with glycerol-gelatin and cover slips, finally examined by light microscopy with the aid of an Olympus BH2 microscope.

RESULTS

VSMC Cultures

The results of mRNA copies/μl obtained by real-time RT-PCR were normalized to PBGD mRNA. PBGD mRNA was detected in all VSMC culture samples analyzed. Mean values of three independent experiments measured in duplicate showed no significant differences in the amount of PBGD-mRNA copies/μl ($P = 0.78$) indicating a non-regulated production of the house-keeping gene during PDGF-incubation. Melting curve analysis with the LC software showed only the expected specific products for all real-time PCR runs in cell culture and human specimens (Fig. 1). Amplification of oligo-dimers or other unspecific products that may interfere with amplification efficiency were not detected. These results were confirmed by gel-electrophoresis of real-time PCR products. Variability of measurements was determined by repeated analysis and showed a variation coefficient between 5 and 10% for the individual LC-PCRs.

Normalized amounts of integrin and ADAM mRNA production in VSMC showed a significant increase under PDGF stimulation over a

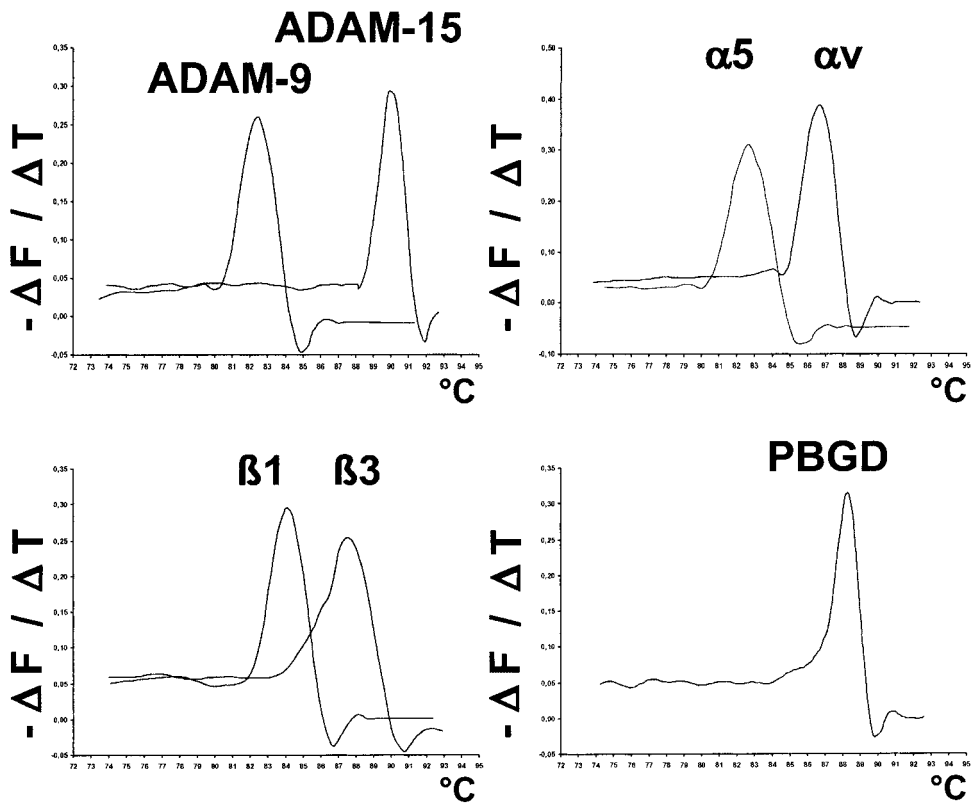

Fig. 1. Melting curve analysis of real-time polymerase chain reaction (PCR) products with the lightcycler (LC) software showed that all real-time PCR runs generated only the expected specific products. No other unspecific products were detected. The graphs show the fluorescence-change (y-axis) per temperature (x-axis) representing a transformation of the melting curve. Two PCR targets are combined in the first three graphs. The presence of a specific product is indicated by a distinct peak between 83°C and 90°C product melting temperature. Gel electrophoresis of real-time RT-PCR products confirmed the absence of unspecific amplification products.

3-day culture period compared to cells cultured without growth factors (Fig. 2): ADAM-9 mRNA was 23-fold increased in arterial VSMC or 25-fold in venous VSMC; ADAM-15 19-fold in arterial and venous VSMC; α5 22-fold in arterial and venous VSMC; β1 sevenfold in arterial and 10-fold in venous VSMC; αv 19-fold in arterial and 21-fold in venous VSMC; β3 11-fold in arterial and 13-fold in venous VSMC. Real-time PCR products electrophoresed on polyacrylamide gels were visualized through ethidium bromide staining (Fig. 3). The intensity of PCR product bands of PDGF-stimulated and non-stimulated arterial and venous VSMC confirmed the quantitative data of real-time PCR. Western blot of arterial and venous VSMC incubated with PDGF for 3 days showed an increased protein expression of ADAM-9, ADAM-15, αvβ3, and α5β1 compared to cells cultured without growth factors (Fig. 4). Bands with typical and identical molecular weight were found for ADAMs and integrins with an increased protein expression in PDGF-stimulated VSMC. For ADAM-15, two distinct bands were demonstrated with molecular weights corresponding to ADAM-15 molecules after cleavage of the pro-domain or the pro- and metalloproteinase-domain [Herren et al., 1997]. α5β1, αvβ3, ADAM-9, and ADAM-15 were produced on a low level by non-stimulated VSMC (Figs. 2–4). This resulted from a low basal production of α5β1, αvβ3, ADAM-9, and ADAM-15 mRNA and protein in the original tissue. This was demonstrated by Western blot and RT-PCR performed on direct extracts of arterial and venous medial tissue used to prepare VSMC cultures (data not shown).

Real-time PCR analysis of VSMC incubated over varying culture periods showed that after a 6-h incubation with PDGF, 10 ng/ml integrin mRNA production was slightly increased. After 12-h incubation, αvβ3 and α5β1 mRNA were significantly increased in arterial and venous VSMC compared to the beginning of incubation (0-h values). ADAM-15 and ADAM-9 mRNA were significantly increased after a 24-h incubation period (Fig. 5). Integrin and ADAM mRNA remained elevated until day 3 of PDGF-incubation.

Atherosclerotic and Normal Human Specimens

mRNA production of ADAM-9, ADAM-15, α5, β1, αv, and β3 in atherosclerotic carotid speci-

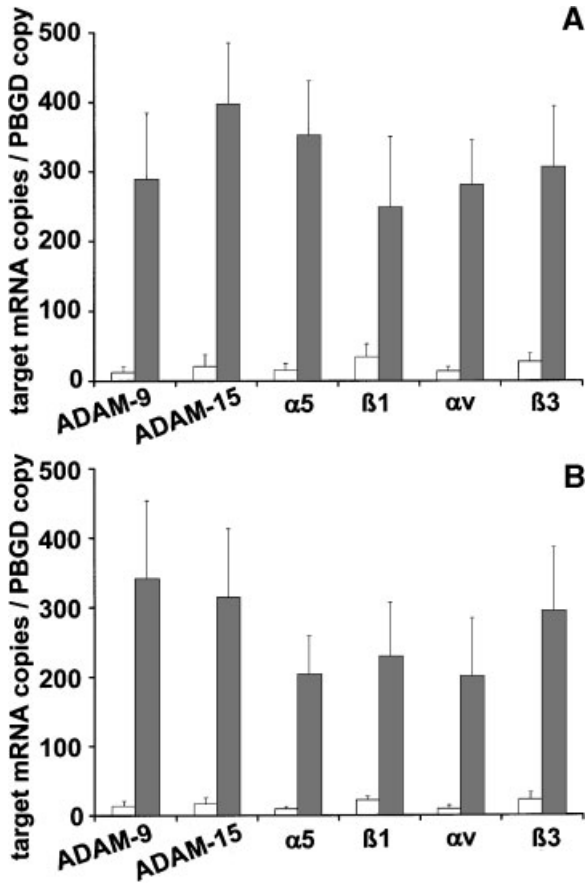

Fig. 2. ADAM-9, ADAM-15, integrin subunits α5, β1, αv, and β3 mRNA production quantified by real-time PCR of VSMC incubated in the absence (white bars) or presence (grey bars) of 10 ng/ml PDGF over a 3-day culture period. The results of arterial VSMC (from human internal mammary artery) are given in (**A**), those of venous VSMC (from human saphenous vein) are given in (**B**). The bars represent mean values of three independent experiments measured in duplicate, reported on the y-axis as normalized amounts of target mRNA copies/1 PBGD-mRNA copy. The thin lines represent the standard error. Differences between PDGF-stimulated and non-stimulated VSMC cultures were significant. In detail, real-time PCR yielded the following results for arterial VSMC cultures incubated in the absence versus in the presence of PDGF (mean values are rounded; standard error values given are in parentheses, the level of significance in student's *t*-test is indicated by the *P*-value): ADAM-9 13 (8.2) versus 289 (96.2) mRNA copies/PBGD copy ($P = 0.02$); ADAM-15 21 (17.4) versus 398 (88.4) mRNA copies/PBGD copy ($P = 0.012$); α5 integrin subunit 16 (9.1) versus 352 (78.6) mRNA copies/PBGD copy ($P = 0.004$); β1 35 (18.1) versus 248 (102.3) mRNA copies/PBGD copy ($P = 0.01$); αv 15 (6.5) versus 280 (65.2) mRNA copies/PBGD copy ($P = 0.005$); β3 28 (11.6) versus 307 (88.2) mRNA copies/PBGD copy ($P = 0.002$). For venous VSMC, the following results were obtained: ADAM-9 14 (7.0) versus 341 (112.3) mRNA copies/PBGD copy ($P = 0.013$); ADAM-15 16 (9.2) versus 315 (97.6) mRNA copies/PBGD copy ($P = 0.022$); α5 integrin subunit 9 (3.4) versus 204 (54.3) mRNA copies/PBGD copy ($P = 0.007$); β1 22 (4.7) versus 230 (78.2) mRNA copies/PBGD copy ($P = 0.001$); αv 9 (4.6) versus 201 (82.6) mRNA copies/PBGD copy ($P = 0.009$); β3 23 (9.6) versus 294 (91.8) mRNA copies/PBGD copy ($P = 0.006$).

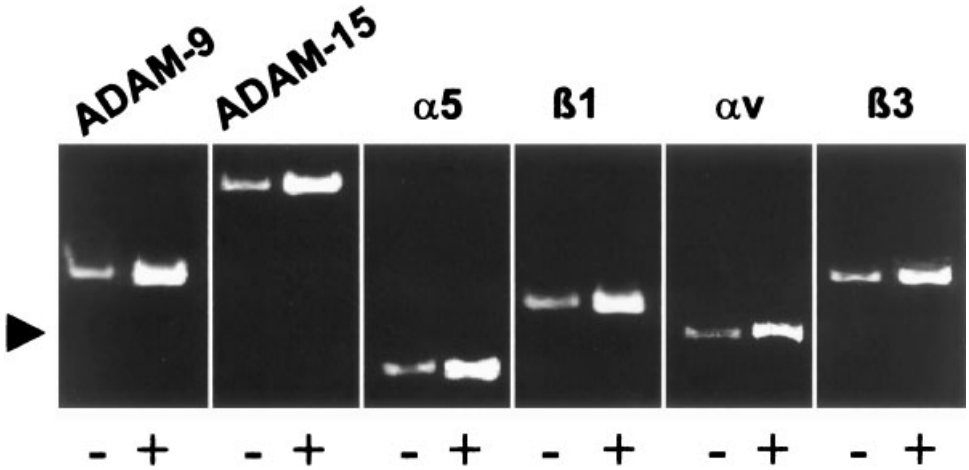

Fig. 3. Ethidium bromide staining of real-time RT-PCR products electrophoresed on 8% native polyacrylamide gels. VSMCs were incubated with (+) or without (−) 10 ng/ml PDGF over a 3-day culture period. Representative PCR products for ADAM-9, ADAM-15, α5, β1, αv, and β3 of non-stimulated and stimulated arterial VSMC from the same experiment are demonstrated. Non-stimulated VSMCs showed a lower intensity of product bands reflecting the lower amounts of mRNA copies demonstrated in Figure 2. Similar results were found for venous VSMC. The expected PCR product lengths were confirmed by a 25-bp ladder. The position of the 100-bp marker is indicated by an arrowhead on the left outer side.

mens quantified by real-time RT-PCR was significantly increased compared to normal specimens (Fig. 6). Mean values of three consecutive measurements showed the following results: mRNA production of ADAM-9 was ninefold, of ADAM-15 sevenfold, of α5 integrin subunit 14-fold, of β1 ninefold, of αv 12-fold, and of β3 fourfold increased in the atherosclerotic group compared to normals. All differences reached statistical significance. In atherosclerotic specimens, all target mRNAs were strongly upregulated. In individual normal specimens, mRNA production of either ADAM-9, ADAM-15, α5, αv, or β3 was absent. PBGD mRNA production was detected in all specimens analyzed without significant differences in the amount of PBGD-mRNA copies/μl between the atherosclerotic versus the normal group ($P = 0.93$; three consecutive real-time PCR measurements). This indicated a non-regulated production of the house-keeping gene. To obtain control arteries reliably unaffected by atherosclerosis, thyroid artery specimens from pre-menopausal women were employed in this study. Thyroid and internal carotid arteries both belong to muscular type arteries. Control tissues from autopsies or artery explants from operations in elderly patients tested in preceding experiments were not suitable because of autolysis or microscopic atherosclerotic changes. Thyroid arteries of patients with diffuse atherosclerosis undergoing thyroid operations showed similar integrin and ADAM changes as the atherosclerotic carotid arteries (data not shown).

No correlation could be detected, when comparing ADAM and integrin mRNA production in atherosclerotic neointima with clinical determinants, such as stage of cerebro-vascular insufficiency, ultrasound or angiography findings, concomitant cardiovascular, metabolic, or malignant disorders, preoperative medication and postoperative complications.

On the protein level, immunohistochemistry showed that ADAM-9 and ADAM-15 were expressed by smooth muscle cells in the neointima of atherosclerotic arteries (Fig. 7). Especially, foam cells of smooth muscle origin and smooth muscle cells surrounding lipidic cores in the neointima prominently expressed ADAM-9 and ADAM-15. Immunostaining for smooth muscle α-actin revealed a predominance of smooth muscle cells in the neointima. CD68 was expressed by individual cells among foam cell accumulations indicating their macrophage origin (data not shown). Integrins α5β1 and αvβ3 were expressed by smooth muscle cells in the neointima and media of atherosclerotic arteries (Fig. 7). The expression patterns of both ADAMs and integrins were mostly congruent in all specimens analyzed, especially the possible binding partners ADAM-15, α5β1, and αvβ3. In normal arteries, immunostaining showed a weak expression of ADAM-9 and ADAM-15 and a moderate expression of αvβ3

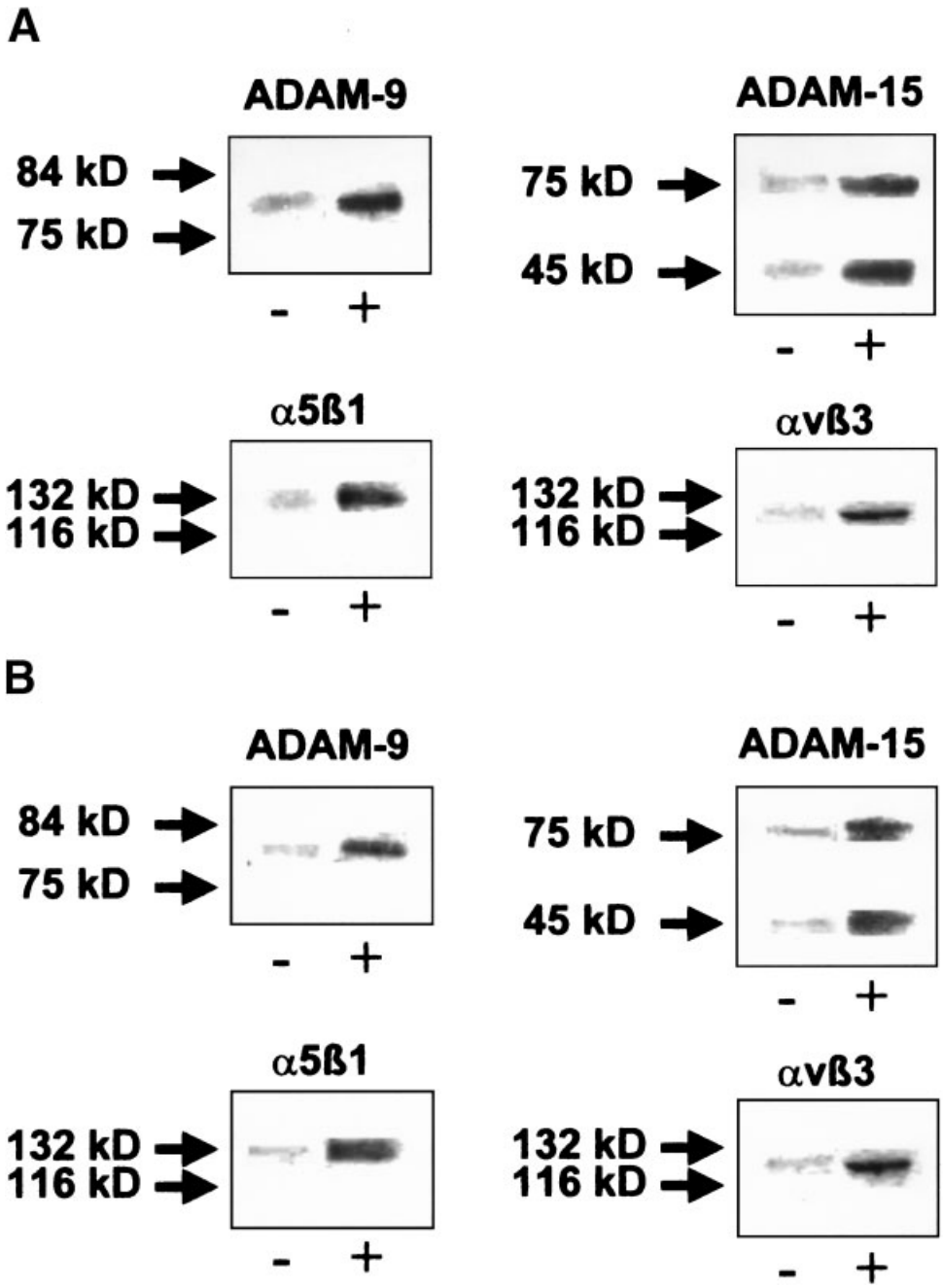

Fig. 4. Integrin and ADAM protein expression of VSMC cultured in the presence (+) or absence (−) of 10 ng/ml PDGF over a 3-day culture period was analyzed by Western blot. The results of arterial VSMC are given in (**A**), those of venous VSMC are given in (**B**). The arrows indicate the position of different molecular weight markers and their weight in kilodaltons. Expression of integrins α5β1, αvβ3, of ADAM-9 and ADAM-15 was increased with PDGF incubation.

in the media (Fig. 7). α5β1 could not be detected on the protein level in normal arteries. Lightmicroscopical examination of conventional stains revealed that all atherosclerotic specimens showed advanced lesion types of neointima development (type IV–VI) [Stary, 1992]. Normal specimens showed no signs of neointima development. The diameter of the whole normal artery wall, measured in a 25-fold magnification, was approximately 400–500 μm. The diameter of the neointima and media of atherosclerotic specimens was approximately

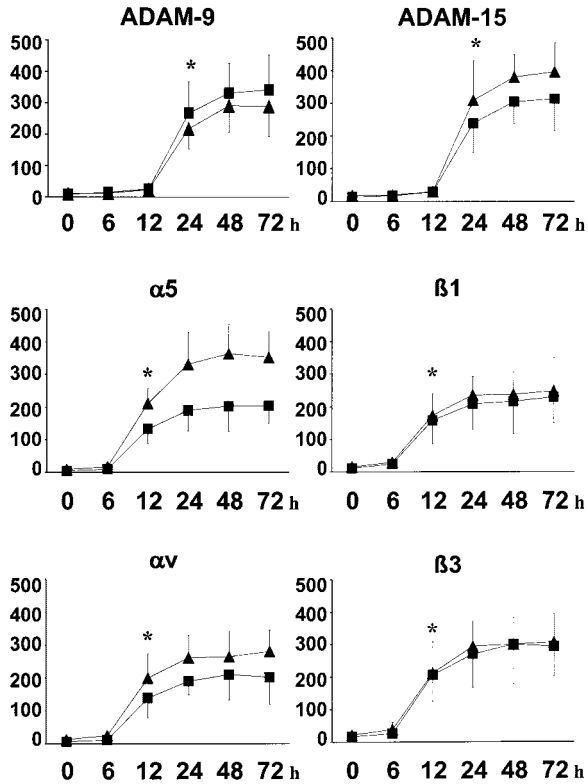

Fig. 5. By means of real-time PCR, integrin and ADAM mRNA production was analyzed at different time points in VSMC culture during incubation with 10 ng/ml PDGF: at 0, 6, 12, 24 h, 2 and 3 days. In the graphs, integrin and ADAM mRNA production of arterial VSMC is marked by triangles, of venous VSMC by squares. The results are reported on the y-axis as target mRNA copies/1 PBGD copy and represent mean values of three independent experiments measured in duplicate. The thin lines indicate the standard error. Significance of differences ($P < 0.05$; *) was reached after 12-h incubation for αv, β3, α5, and β1 mRNA and after 24-h incubation for ADAM-15 and ADAM-9 mRNA compared to the beginning of incubation (0 h) in arterial and venous VSMC. The following results were obtained in arterial VSMC cultures incubated with PDGF over 0, 6, 12, 24 h, 2 and 3 days (rounded mean values; standard errors in parentheses): ADAM-9 10 (4.5), 11 (4.3), 23 (9.9), 217 (66.4), 290 (85.6), 289 (96.2) mRNA copies/PBGD copy; ADAM-15 18 (10.3), 20 (9.7), 31 (14.6), 310 (120.3), 381 (70.2), 398 (88.4) mRNA copies/PBGD copy; α5 integrin subunit 8 (3.2), 16 (8.7), 211 (45.7), 331 (99.7), 364 (89.9), 352 (78.6) mRNA copies/PBGD copy; β1 16 (7.6), 29 (13.2), 174 (65.6), 236 (56.8), 238 (67.9), 248 (102.3) mRNA copies/PBGD copy; αv 12 (8.3), 25 (10.1), 199 (74.8), 261 (69.5), 264 (78.4), 280 (65.2) mRNA copies/PBGD copy; β3 22 (9.9), 39 (21.2), 212 (95.6), 294 (78.2), 300 (82.9), 307 (88.2) mRNA copies/PBGD copy. In venous VSMC cultures, the following results were obtained: ADAM-9 9 (2.3), 15 (5.6), 26 (9.7), 266 (101.2), 331 (94.6), 341 (112.3) mRNA copies/PBGD copy; ADAM-15 14 (5.7), 18 (10.3), 30 (11.6), 239 (89.7), 306 (66.8), 315 (97.6) mRNA copies/PBGD copy; α5 integrin subunit 4 (1.9), 9 (3.7), 133 (44.7), 190 (64.1), 203 (78.4), 204 (54.3) mRNA copies/PBGD copy; β1 11 (4.6), 24 (11.0), 159 (72.0), 209 (80.4), 217 (99.7), 230 (78.2) mRNA copies/PBGD copy; αv 7 (3.3), 12 (5.7), 139 (60.2), 189 (41.0), 210 (76.8), 201 (82.6) mRNA copies/PBGD copy; β3 17 (7.8), 26 (8.8), 206 (80.1), 270 (103.0), 300 (120.3), 294 (91.8) mRNA copies/PBGD copy.

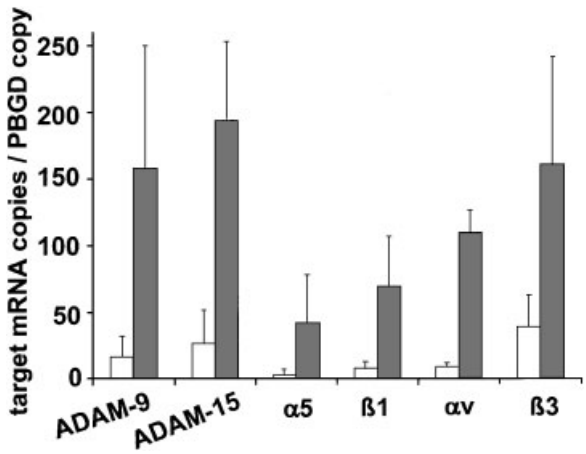

Fig. 6. Integrin and ADAM mRNA production of eight normal (white bars) and 13 atherosclerotic (grey bars) human artery specimens was quantitated by real-time PCR. The bars represent mean values of three consecutive measurements of all specimens of each group, reported as normalized amounts of target mRNA copies/1 PBGD-mRNA copy. The thin lines represent the standard error of interpatient differences. mRNA production of normal and atherosclerotic specimens is compared for every target; differences between normal and atherosclerotic specimens were significant. In detail, real-time PCR yielded the following results for normal versus atherosclerotic specimens (rounded mean values; standard error, and *P*-value in parentheses): ADAM-9 17 (15.3) versus 158 (92.1) mRNA copies/PBGD copy ($P = 0.018$); ADAM-15 27 (24.5) versus 194 (59.2) mRNA copies/PBGD copy ($P = 0.03$); α5 integrin subunit 3 (4.5) versus 42 (35.6) mRNA copies/PBGD copy ($P = 0.008$); β1 8 (4.8) versus 69 (37.2) mRNA copies/PBGD copy ($P = 0.001$); αv 9 (1.5) versus 109 (16.5) mRNA copies/PBGD copy ($P = 0.027$); β3 38 (24.3) versus 160 (81.3) mRNA copies/PBGD copy ($P = 0.001$).

1,200–2,400 μm, resulting mainly from a broad neointima measuring 1,000–2,200 μm. In normal arteries, only the media contained smooth muscle cells, macrophages were absent in the vessel wall (data not shown). Immunostaining for T-lymphocyte antigen CD3 and B-lymphocyte antigen CD21 showed no reactivity in (neo)intima or media of atherosclerotic and normal arteries (data not shown). Specificity of all immunostaining reactions was verified through negative controls.

DISCUSSION

During neointima formation, the regulation of cell–matrix interactions is profoundly altered, mainly through changes in the expression, cell surface density, and ligand affinity of integrins. The integrins αvβ3 and α5β1, involved in smooth muscle cell migration and proliferation, influence neointima growth [Kim and Yamada, 1997; Moiseeva, 2001]. αvβ3

disinhibits cell migration and proliferation, α5β1 is involved in cell migration, proliferation, and blood vessel repair, as well as in fibrin clot contraction [Moiseeva, 2001]. Both integrins cooperate in the migration of smooth muscle cells to sites of vascular injury [Ikari et al., 2000]. Counter-regulatory mechanisms balancing these processes are, among others, integrin binding through different ligands [Kim and Yamada, 1997; Isacke and Horton, 2000; Moiseeva, 2001]. ADAMs have been proposed as integrin regulators [Blobel, 1997; Herren et al., 1997; Stone et al., 1999; Nath et al., 1999, 2000]. In this study, RNA and protein production of integrins αvβ3 and α5β1, of ADAM-9 and ADAM-15 in VSMC cultures, normal and atherosclerotic vessels was analyzed to demonstrate parallel or sequential expression changes. Concurrent regulation of integrins and cell-bound disintegrins has not been investigated previously. A related regulation of integrins and ADAMs would support the proposed integrin-regulating function of ADAMs.

Integrins α5β1, αvβ3, ADAM- 15, and ADAM-9 were strongly increased in VSMC of arterial and venous origin after PDGF-incubation for 3 days (Figs. 2 and 4). PDGF is a potent stimulator of smooth muscle cell migration and proliferation in cell culture and in vivo. It promotes neointima growth by inducing smooth muscle cell accumulation in the neointima [Raines et al., 2000]. The dosage of PDGF-BB used in this study may be reached systemically in patients with acute coronary syndromes [Nilsson et al., 1992]. In previous studies [Huang et al., 2002], we found that PDGF-BB 10 ng/ml induces a strong growth of the neointima in venous and arterial vessel organ cultures with an increase in elastic fibers, cell migration, and proliferation. In the present study, β1 and β3 mRNA of arterial and venous VSMCs were comparably increased through PDGF-incubation. α5 subunit mRNA was also increased by PDGF in VSMC, as supported by other authors [Janat et al., 1992]. The ratio of β1 to β3 integrin expression is dependent on the cell type and proliferation rate [Davenpeck et al., 2001; Moiseeva, 2001]. Several cell types showed a predominance of β3 over β1 integrins on the protein and mRNA level, such as quiescent and stimulated fibroblasts [Kawano et al., 2000], PDGF-stimulated VSMC [Janat et al., 1992], and coronary VSMC [Davenpeck et al., 2001]. Other cell types showed higher levels of β1 integrins, such as aortic VSMC [Yee et al., 1998] and carotid VSMC [Davenpeck et al., 2001]. The expression of β-integrins in the present study may have been influenced by growth factor-induced proliferation and the vascular origin of VSMC. Analysis of integrin mRNA production at different time points during PDGF-incubation revealed that α5β1 and αvβ3 mRNA were significantly increased after 12-h incubation in arterial and venous VSMC compared to the start of incubation (Fig. 5). The time course of integrin expression is supported by findings on αvβ3 expression in fibroblast cell culture [Graf et al., 2000] and an animal model [Corjay et al., 1999]. In contrast, a more rapid increase in αvβ3 mRNA 6 h after PDGF-incubation and no detectable αvβ3 mRNA 24 h after stimulation has been observed in rabbit VSMC [Janat et al., 1992]. Differences in intracellular signal transduction varying with the cell type and the quality of the intracellular signal [Heldin et al., 1998] may account for these discrepancies. The time lag between growth factor receptor ligation and increased integrin gene expression could result from varying responses of the signal transduction cascade [Heldin et al., 1998].

Fig. 7. Immunohistochemistry of atherosclerotic carotid artery (left column, 200-fold magnification) and of normal thyroid artery (right column, 400-fold magnification), visualized through streptavidin-alkaline phosphatase-conjugate, Fast Red stain (red arrows in (**A**) point to positive reactions) and Mayer's hemalum counterstain. The endothelium (luminal border) of normal and atherosclerotic arteries is indicated by black arrows (**A**, **B**). Black arrowheads point to the border of the intima or the neointima with the media. Photomicrographs of serial sections comparing the expression of ADAM-9 in atherosclerotic (**A**) and normal (**B**) arteries, of ADAM-15 (**C**, **D**), integrins α5β1 (**E**, **F**), and αvβ3 (**G**, **H**). Note the broad neointimal area between the endothelium and the remainders of the lamina elastica interna (black arrowheads in (**A**) in the atherosclerotic sections. Normal arteries were free of any sign of neointima formation; note the thin intima and uninterrupted lamina elastica interna (**B**). ADAM-9, ADAM-15, α5β1, and αvβ3 were prominently expressed by smooth muscle cells in the neointima of atherosclerotic arteries. Both ADAMs and integrins were predominantly expressed in regions of smooth muscle cell accumulation in the surrounding of lipidic cores. In these areas, only individual macrophages were found (data not shown). In normal arteries, ADAM-9 and ADAM-15 showed a weak expression, αvβ3 a moderate expression in the media. α5β1 could not be demonstrated on the protein level in normal arteries. The scale bars in panels **G** and **H** represent 100 μm.

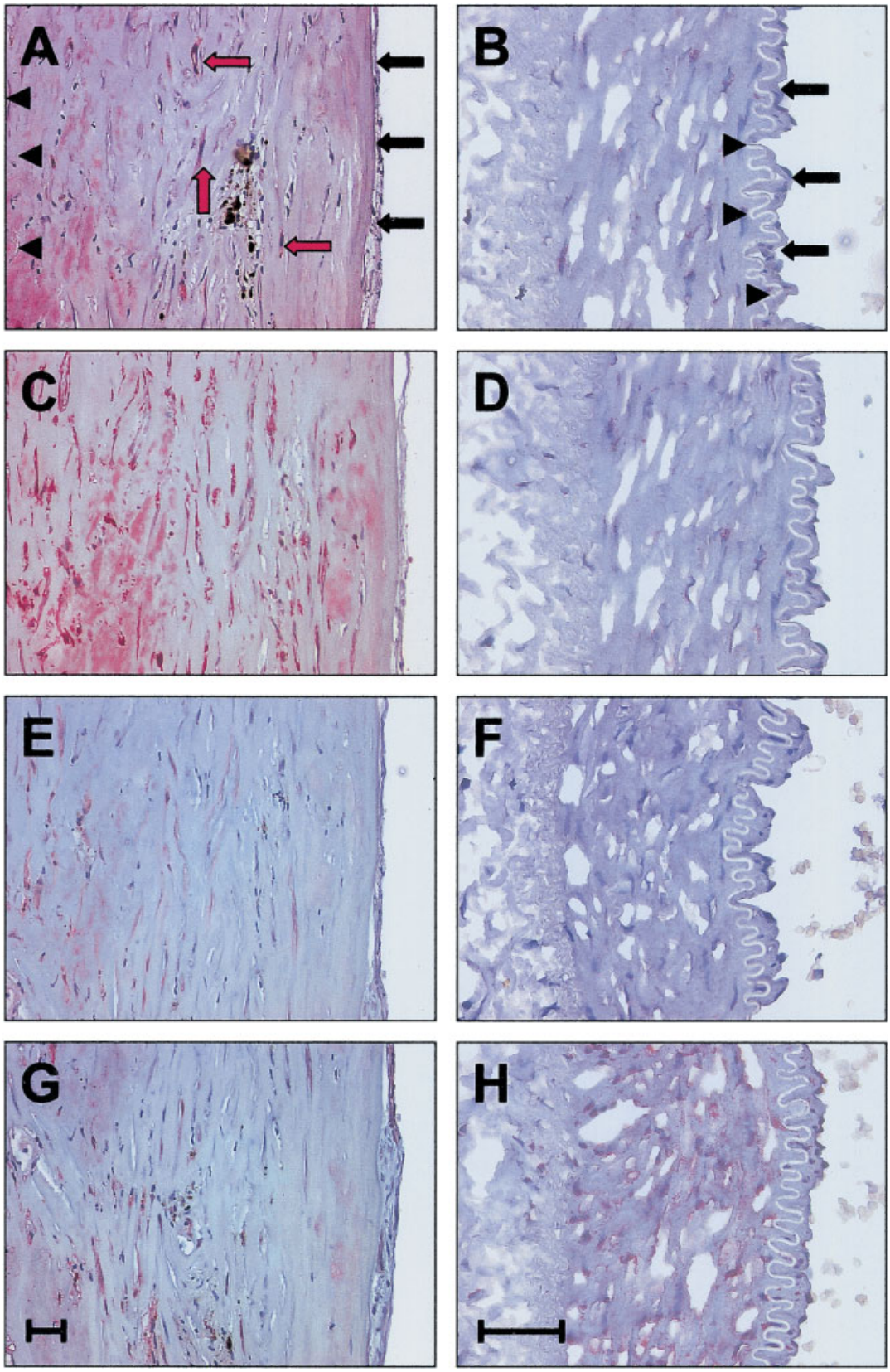

Fig. 7.

ADAM-15 and ADAM-9 mRNA were significantly increased after 24-h incubation and remained elevated during the 3-day incubation period (Fig. 5). Pronounced expression of both ADAMs has previously been demonstrated in various leucaemic cell lines suggesting a role in haematological malignancies [Wu et al., 1997]. In a model of inflammation in cultured chondrocytes, differential regulation of ADAM-9 and ADAM-15 has been observed [Flannery et al., 1999]. This had prompted us to investigate ADAM-9 expression next to ADAM-15, the latter being a ligand of integrins α5β1 and αvβ3 [Nath et al., 1999]. However, in atherosclerosis, ADAM-9 was not found to be downregulated as in inflammatory processes, rather upregulated together with ADAM-15. ADAM-15 expression has previously been demonstrated in the atherosclerotic aorta of non-human primates and in human aortic VSMC [Herren et al., 1997]. ADAM-15 mRNA was not found to be upregulated by PDGF 1 nM or 55 ng/ml in VSMC during a 120-min incubation period [Herren et al., 1997] (compared to 10 ng/ml or 0.2 nM in the present study). The increased ADAM-15 expression in the present study was, therefore, probably not a direct effect of PDGF. PDGF transmits mitogenic and migration-promoting signals through the PDGF-receptors to intracellular signal transduction cascades involving various kinases and signal transduction molecules [Heldin et al., 1998]. These intracellular targets activate other signal transduction molecules that lead to changes in integrin, possibly also ADAM activity or gene expression. PDGF affects integrin αvβ3- and α5β1-mediated migration or adhesion through phosphatidylinositol 3-kinase, protein-kinase C family [Baron et al., 2002], calcium/calmodulin-dependent protein kinase II [Bilato et al., 1997], or extracellular signal-regulated kinase [Berrou and Bryckaert, 2001]. PDGF also induces integrin gene expression [Heldin et al., 1998], for example β1-integrin expression, through a protein-kinase C-zeta dependent pathway [Xu et al., 1996]. These cellular responses to PDGF require several hours [Heldin et al., 1998; Baron et al., 2002]. A direct and rapid communication of PDGF-signals within less than 1 h affects mainly integrin avidity transferred through focal adhesion kinase to the integrins [Sieg et al., 2000]. ADAM- 15 and ADAM-9 mRNA were upregulated in a time interval of 24 h after PDGF-stimulation following integrins α5β1 and αvβ3. Upregulation of ADAMs may occur reactively to increased integrin expression to modulate integrin–matrix interactions. Intracellular signaling cascades connecting growth factor and ADAM signal transduction pathways are still undefined. PDGF-stimulation of extracellular signal-regulated kinase activity was not influenced by ADAM-15 [Herren et al., 2001]; however, other pathways may be involved. The cytoplasmic domain of ADAMs takes part in signal transduction and is suggested to alter cellular activation [Weskamp et al., 1996; Herren et al., 1997; Howard et al., 1999]. Signal transduction cascades that induce ADAM gene expression following integrin gene expression, as demonstrated in this study, remain to be elucidated.

In human specimens, ADAM-9 and ADAM-15 mRNA similarly showed a low production in normal arteries and a significant increase in atherosclerotic arteries. Integrin α5β1 and αvβ3 mRNA showed a strong upregulation in atherosclerotic arteries comparable to ADAMs mRNA upregulation. There was a low production of α5, αv, and β1 integrin subunits and a moderate production of β3 in normals (Fig. 6). ADAMs and integrins were prominently expressed by smooth muscle cells in the neointima with a similar distribution, as demonstrated by immunostaining. In contrast, normal arteries showed a low integrin and ADAM expression (Fig. 7). The expression of α5β1, αvβ3, and ADAM-15 in atherosclerotic compared to normal arteries is consistent with the results of other authors [Hoshiga et al., 1995; Herren et al., 1997; Hillis et al., 1998; Veinot et al., 1999]. ADAM-9 has not been investigated previously in arteries. Atherosclerotic and normal artery specimens contained higher levels of β3 than β1 mRNA. A slight predominance of αvβ3 in normal arteries was also found by immunohistochemistry, though expression levels of β-integrins mRNA and protein were low. A predominance of β3 over β1 integrins has been described, but also higher levels of β1 or variable ratios depending on the cell type [Janat et al., 1992; Yee et al., 1998; Kawano et al., 2000; Davenpeck et al., 2001]. β-integrin expression ratios may differ with the size and type of the investigated artery [Yee et al., 1998; Davenpeck et al., 2001]. The clinical implications of changes in integrin and ADAM expression demonstrated in this study are yet to be determined, since we could not find a correla-

tion with patient data. The number of patients included in this study may have reduced statistical evidence.

The molecular structure of ADAMs and functions of their various domains give explanations for the parallel upregulation with integrins. The disintegrin-domain contains an integrin-binding sequence varying in the amino acid sequence between the different ADAMs [Wolfsberg et al., 1995; Stone et al., 1999]. The metalloproteinase-domain exhibits zinc-dependent metalloproteinase- and proteinase-activity [Stone et al., 1999]. ADAM-9 and ADAM-15 may cleave cell–matrix bonds through the metalloproteinase-domain to support cell migration [Herren et al., 1997; Loechel et al., 1998; Flannery et al., 1999; Roghani et al., 1999]. The metalloproteinase-domain may be proteolytically released from the cell-bound ADAM molecule to function as a free protease [Herren et al., 1997]. In the present study, ADAM-15 was found in two molecular weight forms in Western blot (Fig. 4), corresponding to molecules after cleavage of the pro- or metalloproteinase-domain [Herren et al., 1997]. Due to its molecular structure, ADAM-9 is believed to have an inhibitory effect on cellular activation [Wolfsberg et al., 1995; Flannery et al., 1999; Stone et al., 1999]. In the context of this study, especially the integrin-binding or -regulating function of the disintegrin-domain and the migration-promoting function of the metalloproteinase-domain make ADAM-15 and ADAM-9 ideal candidates as adhesion- and migration-regulating molecules. Increased expression of ADAM-15 reduces migration and intensifies intercellular adhesion [Herren et al., 2001]. Binding of $\alpha v\beta 3$ or $\alpha 5\beta 1$ through ADAM-15 [Zhang et al., 1998; Nath et al., 1999] could modulate the migration-and proliferation-promoting effect of these integrins on smooth muscle cells [Moiseeva, 2001]. In contrast, binding of ADAM-15 to the primary fibronectin receptor $\alpha 5\beta 1$ [Nath et al., 1999] could facilitate migration, since interaction between $\alpha 5\beta 1$ and fibronectin supresses migration [Werb et al., 1989]. Taken together, ADAM-9 and ADAM-15 may have migration-promoting [Nath et al., 2000], but also -inhibiting functions.

In conclusion, ADAM-9 and ADAM-15 seem to be upregulated following an increased expression of integrins $\alpha 5\beta 1$ and $\alpha v\beta 3$ in atherosclerosis. The altered expression of ADAMs may be a reaction to a changed balance of integrins and extracellular matrix proteins during neointima formation. We suggest that in atherosclerosis, ADAMs are capable of functioning as integrin regulators, allowing cells to specifically open or block integrin binding to various ligands, thereby orchestrating cell–cell and cell–matrix interactions, migration, and proliferation. Finding the key events leading to neointima formation depends on a better understanding of the regulatory mechanisms of integrin function. Future directions should include a detailed analysis of the interactions of different ADAMs with integrins and their influence on cell migration in atherosclerosis. These investigations may eventuate into new targets to control neointima formation.

ACKNOWLEDGMENTS

The authors thank M. Philipp, S. Scheffler, and O. Dakischew for valuable technical assistance.

REFERENCES

Al-Fakhri N, Yu JCM, Paul M, Buhr HJ. 1997. Significance of endothelin for neointima formation and neovascularization in peripheral arterial occlusive disease. Langenbecks Arch Chir Suppl 97/I:25–28.

Baron W, Shattil SJ, ffrench-Constant C. 2002. The oligodendrocyte precursor mitogen PDGF stimulates proliferation by activation of αvß3 integrins. EMBO J 21: 1957–1966.

Berrou E, Bryckaert M. 2001. Platelet-derived growth factor inhibits smooth muscle cell adhesion to fibronectin by ERK-dependent and ERK-independent pathways. J Biol Chem 276:39303–39309.

Bilato C, Curto KA, Monticone RE, Pauly RR, White AJ, Crow MT. 1997. The inhibition of vascular smooth muscle cell migration by peptide and antibody antagonists of the αvß3 integrin complex is reversed by activated calcium/calmodulin-dependent protein. J Clin Invest 100:693–704.

Blobel CP. 1997. Metalloprotease-disintegrins: Links to cell adhesion and cleavage of TNF-α and notch. Cell 90:589–592.

Chomczynski P, Sacchi N. 1987. Single-step method of RNA isolation by acid guanidinium thiocyanate-phenol-chloroform extraction. Anal Biochem 162:156–159.

Corjay MH, Diamond SM, Schlingmann KL, Gibbs SK, Stoltenborg JK, Racanelli AL. 1999. αvß3, αvß5, and osteopontin are coordinately upregulated at early time points in a rabbit model of neointima formation. J Cell Biochem 75:492–504.

Davenpeck KL, Marcinkiewicz C, Wang D, Niculescu R, Shi Y, Martin JL, Zalewski A. 2001. Regional differences in integrin expression: Role of α5ß1 in regulating smooth muscle cell functions. Circ Res 88:352–358.

Eto K, Puzon-McLaughlin W, Sheppard D, Sehara-Fujusawa A, Zhang XP, Takada Y. 2000. RGD-independent binding of integrin α9ß1 to the ADAM-12 and -15

disintegrin domains mediates cell–cell interaction. J Biol Chem 275:34922–34930.

Flannery CR, Little CB, Caterson B, Hughes CE. 1999. Effects of culture conditions and exposure to catabolic stimulators (IL-1 and retinoic acid) on the expression of matrix metalloproteinases (MMPs) and disintegrin metalloproteinases (ADAMs) by articular cartilage chondrocytes. Matrix Biol 18:225–237.

Graf K, Neuss M, Stawowy P, Hsueh WA, Fleck E, Law RE. 2000. Angiotensin II and αvß3 integrin expression in rat neonatal cardiac fibroblasts. Hypertension 35:978–984.

Hanaki K, Nakatake H, Yamamoto K, Odawara T, Yoshikura H. 2000. DNAse I activity retained after heat inactivation in standard buffer. BioTechniques 29: 38–42.

Heldin CH, Ostman A, Ronnstrand L. 1998. Signal transduction via platelet-derived growth factor receptors. Biochim Biophys Acta 1378:F79–F113.

Herren B, Raines EW, Russel R. 1997. Expression of a disintegrin-like protein in cultured human vascular cells and in vivo. FASEB J 11:173–180.

Herren B, Garton KJ, Coats S, Bowen-Pope DF, Ross R, Raines EW. 2001. ADAM15 overexpression in NIH3T3 cells enhances cell–cell interactions. Exp Cell Res 271: 152–160.

Hillis GS, Mlynski RA, Simpson JG, MacLeod AM. 1998. The expression of ß1 integrins in human coronary artery. Basic Res Cardiol 93:295–302.

Hoshiga M, Alpers CE, Smith LL, Giachelli CM, Schwartz SM. 1995. αvß3 integrin expression in normal and atherosclerotic artery. Circ Res 77:1129–1135.

Howard L, Nelson KK, Maciewicz RA, Blobel CP. 1999. Interaction of the metalloprotease disintegrins MDC9 and MDC15 with two SH3 domain-containing proteins, endophilin I and SH3PX1. J Biol Chem 274:31693–31699.

Huang TF. 1998. What have snakes taught us about integrins? Cell Mol Life Sci 54:527–540.

Huang B, Dreyer T, Heidt M, Yu JC, Philipp M, Hehrlein FW, Katz N, Al-Fakhri N. 2002. Insulin and local growth factor PDGF induce intimal hyperplasia in bypass graft culture models of saphenous vein and internal mammary artery. Eur J Cardiothorac Surg 21:1002–1008.

Huovila APJ, Almeida EAC, White JM. 1996. ADAMs and cell fusion. Curr Opin Cell Biol 8:692–699.

Ikari Y, Yee KO, Schwartz SM. 2000. Role of α5ß1 and αvß3 integrins on smooth muscle cell spreading and migration in fibrin gels. Thromb Haemost 84:701–705.

Isacke C, Horton M. 2000. The adhesion molecule facts book. 2nd edition. London-San Diego: Academic Press. p 9–12, 158–164, 181–183.

Janat MF, Argraves WS, Liau G. 1992. Regulation of vascular smooth muscle cell integrin expression by transforming growth factor beta1 and by platelet-derived grwoth factor-BB. J Cell Physiol 151:588–595.

Kawano H, Cody RJ, Graf K, Goetze S, Kawano Y, Schnee J, Law RE, Hsueh WA. 2000. Angiotensin II enhances integrin and alpha-actinin expression in adult rat cardiac fibroblasts. Hypertension 35:273–279.

Kim LT, Yamada KM. 1997. The regulation of expression of integrin receptors. Proc Soc Exp Biol Med 214:123–131.

Loechel F, Gilpin BJ, Engvall E, Albrechtsen R, Wewer UM. 1998. Human ADAM 12 (meltrin α) is an active metalloprotease. J Biol Chem 273:16993–16997.

Moiseeva EP. 2001. Adhesion receptors of vascular smooth muscle cells and their functions. Cardiovasc Res 52:372–386.

Nath D, Slocombe PM, Stephens PE, Warn A, Hutchinson GR, Yamada KM, Docherty AJ, Murphy G. 1999. Interaction of metargidin (ADAM-15) with αvß3 and α5ß1 integrins on different haemopoietic cells. J Cell Sci 112:579–587.

Nath D, Slocombe PM, Webster A, Stephens PE, Docherty AJ, Murphy G. 2000. Meltrin gamma (ADAM-9) mediates cellular adhesion through α6ß1 integrin, leading to a marked induction of fibroblast cell motility. J Cell Sci 113:2319–2328.

Nilsson J, Volk-Jovinge S, Svensson J, Landou C, De-Faire U, Hamsten A. 1992. Association between high levels of growth factors in plasma and progression of coronary atherosclerosis. J Intern Med 232:397–404.

Raines EW, Koyama H, Carragher NO. 2000. The extracellular matrix dynamically regulates smooth muscle cell responsiveness to PDGF. Ann NY Acad Sci 902: 39–52.

Roghani M, Becherer JD, Moss ML, Atherton RE, Erdjument-Bromage H, Arribas J, Blackburn RK, Weskamp G, Tempst P, Blobel CP. 1999. Metalloprotease-disintegrin MDC9: Intracellular maturation and catalytic activity. J Biol Chem 274:3531–3540.

Sieg DJ, Hauck CR, Ilic D, Klingbeil CK, Schaefer E, Damsky CH, Schlaepfer DD. 2000. FAK integrates growth-factor and integrin signals to promote cell migration. Nat Cell Biol 2:249–256.

Stary HC. 1992. Composition and classification of human atherosclerotic lesions. Virchows Arch A Pathol Anat Histopathol 421:277–290.

Stone AL, Kroeger M, Sang QXA. 1999. Structure–function analysis of the ADAM family of disintegrin-like and metalloprotease-containing proteins. J Prot Chem 18: 447–465.

Veinot JP, Srivatsa S, Carlson P. 1999. ß3 integrin—a promiscous integrin involved in vascular pathology. Can J Cardiol 15:762–770.

Werb Z, Tremble PM, Behrendtsen O, Crowley E, Damsky CH. 1989. Signal transduction through the fibronectin receptor induces collagenase and stromelysin gene expression. J Cell Biol 109:877–889.

Weskamp G, Kratzschmar J, Reid MS, Blobel CP. 1996. MDC9, a widely expressed cellular disintegrin containing cytoplasmic SH3 ligand domains. J Cell Biol 132: 717–726.

Wiame I, Remy S, Swennen R, Sagi L. 2000. Irreversible heat inactivation of DNAse I without RNA degradation. BioTechniques 29:252–256.

Wilhelm J, Hahn M, Pinguod A. 2000. Influence of DNA target melting behavior on real-time PCR quantification. Clin Chem 46:1738–1743.

Wolfsberg TG, Primakoff P, Myles DG, White JM. 1995. ADAM, a novel family of membrane proteins containing a disintegrin- and metalloprotease-domain: Multipotential functions in cell–cell and cell–matrix interactions. J Cell Biol 131:275–278.

Wu E, Croucher PI, McKie N. 1997. Expression of members of the novel membrane linked metalloproteinase family ADAM in cells derived from a range of haematological malignancies. Biochem Biophys Res Commun 235:437–442.

Xu J, Zutter MM, Santoro SA, Clark RA. 1996. PDGF induction of alpha 2 integrin gene expression is mediated by protein kinase C-zeta. J Cell Biol 134:1301–1311.

Yee KO, Rooney MM, Giachelli CM, Lord ST, Schwartz SM. 1998. Role of ß1 and ß3 integrins in human smooth muscle cell adhesion to and contraction of fibrin clots in vitro. Circ Res 83:241–251.

Zhang XP, Kamata T, Yokoyama K, Puzon-McLaughlin W, Takada Y. 1998. Specific interaction of the recombinant disintegrin-like domain of MDC-15 (metargidin, ADAM-15) with integrin αvß3. J Biol Chem 273:7345–7350.

Zhou M, Graham R, Russell G, Croucher PI. 2001. MDC-9(ADAM-9/Meltrin gamma) functions as an adhesion molecule by binding the αvß5 integrin. Biochem Biophys Res Comm 280:574–580.